Functionalization of High Frequency SAW RFID Devices for Ozone Dosimetry

Ryan S. Westafer*, Galit Levitin†, Dennis W. Hess†, Michael H. Bergin‡, Peter J. Edmonson§, and William D. Hunt*¶
*School of Electrical and Computer Engineering
Georgia Institute of Technology, Atlanta, Georgia 30332–0250, USA
Email: ryan.westafer@gatech.edu
†School of Chemical and Biomolecular Engineering
Georgia Institute of Technology, Atlanta, Georgia 30332, USA
‡School of Environmental Engineering
Georgia Institute of Technology, Atlanta, Georgia 30332, USA
§Zen Sensing, LTD
¶Corresponding author: bill.hunt@ece.gatech.edu

***Abstract*—In this paper we report new work on the gravimetric detection of ozone at EPA and OSHA relevant concentrations (approximately 100 ppb) in filtered ambient air. We have extended our proof-of-concept work which used both quartz crystal microbalance (QCM) and surface acoustic wave (SAW) resonators. We now enable detection using our high frequency SAW RFID devices. Such surface wave devices are extremely sensitive to the viscosity, thickness, and uniformity of the reactive or sorbent coating. We report laboratory characterization of our polymer-coated SAW sensors operating between 200 and 600 MHz on lithium niobate substrates. Return loss measurements confirm adequate load bearing even at 550 MHz. We compare both the temperature and ozone sensitivity of the RFID devices to conventional resonators. In conclusion, we suggest the design improvements to yield a next generation of SAW RFID ozone sensors with even greater sensitivity.**

I. Introduction

Recently, surface acoustic wave devices have been employed as passive wireless sensors. These radio frequency identification (RFID) devices sense environmental perturbations, typically temperature and/or pressure [1], through mechanical changes in the substrate material. Desiring similar functionality for ambient ozone monitoring, we prepared SAW RFID devices with polybutadiene (PB) coatings. After some refinement and validation trials, our results show ozone detection at low concentrations relevant to environmental and occupational regulations.

A. Ozone Standards and Measures

On March 12, 2008 the United States EPA revised the national air quality standards (NAAQS), reducing the "eight hour primary ozone standard" to 75 ppb (parts-per-billion). The Occupational Safety & Health Administration (OSHA) has published a maximum allowable permissible exposure limit at 100 ppb over 8 hours. In New Zealand, "alert" category ozone threshold is reached at 47 ppb, and "action" category is above 70 ppb. These are 1 hour averages published by the Ministry for the Environment (2002). There is an international interest in detection of ambient ozone in the ppb range.

In addition to its production in the atmosphere, ozone is commonly produced indoors by ultraviolet lamps and electric machinery such as photocopiers and arcing in brushed motors. This form of pollution occurs in workplaces around the world. Because toxicity has been reported at concentrations as low as 100 ppb, wireless personal exposure monitoring could be of great benefit.

The dosimeter modality is particularly advantageous for personal exposure monitoring. While one probably could not carry most photometric monitors on the person, a simple single-chip SAW RFID badge can easily accompany a person throughout a workday much as radiation badges and RFID access cards are presently worn or carried by employees.

Continuous online monitoring of ozone is typically performed by photometric gas analyzers, particularly using ultraviolet (UV) spectrophotometry. This method is known to be very precise and very good accuracy may be obtained, even over long range optical atmospheric measurements [2]. However, confounding factors can complicate tropospheric (low-altitude) spectroscopic measurements: SO_2 concentration and varying background UV intensity (e.g. reflected sunlight, clouds, etc.) [3], [4]. We employ a method which enables SAW sensors to detect ozone by its chemical reactivity rather than its optical resonance.

B. Acoustic Ozone Sensing

Acoustic gravimetric ozone sensors were reported in 1985 by Fog et al. [5]. That work used quartz crystal microbalance (QCM) sensors coated with an alkene polymer (polybutadiene) which demonstrated mass increase after ozone reaction. The frequency dependence of acoustic resonators due to mass loading is well known. Density or temperature changes and other factors alter the acoustic velocity. In one view, the characteristic time ($\tau_0 = 1/f_0$) of a resonator is increased by mass adsorption to its free surface. We performed similar proof-of-concept experiments with our coatings on 10 MHz QCM resonators [6]. An example sensitivity plot is shown in

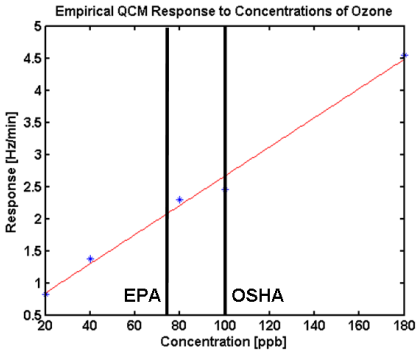

Fig. 1. Quartz resonator results demonstrate suitability of polybutadiene coatings for acoustic gravimetric ozone detection at 10 MHz and within a relevant range.

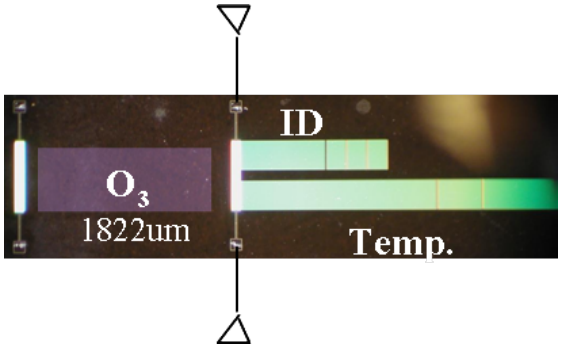

Fig. 2. Optical micrograph of our highest frequency STW mode device (64° Y-X $LiNbO_3$) patterned by electron beam lithography. Annotations indicate the acoustic signal paths and interconnect for future antenna attachment.

figure 1, and it shows operation both above and below the regulatory concentrations.

Makers of SAW RFID tags utilize this velocity dependence to read out remote environmental conditions. Though the devices are not designed as resonators, acoustic velocity changes are still manifest in the arrival times of pulses (a common coding scheme). These SAW RFID devices typically operate in the megahertz range or even low gigahertz frequencies to increase available bandwidth and to reduce antenna dimensions.

In our experiments, we functionalized our SAW RFID devices for operation at frequencies more than one order of magnitude greater than in the QCM studies. Surface preparations which are troublesome (homogeneity) at fractions of 1 GHz would become prohibitively difficult at 2.45 GHz used by some SAW RFID devices [7]). A further complication is that loss is critical in these wireless devices which already suffer r^{-4} free-space propagation loss and piezoelectric coupling (k^2) less than 15%. By reciprocity this implies an ideal return loss of $10\log_{10}(0.15^2) \approx -16$ dB at zero read-out distance ($\mathrm{r} = 0$).

II. Device Design

Several researchers have recently developed SAW RFID sensors for remote detection of temperature, pressure, etc. [8], [1]. Similarly, we have prepared such devices to detect ozone in air.

There is a necessary trade-off between frequency of operation and the mass/thickness of a surface film. For example, the polybutadiene (PB) films used in this work introduce losses at high frequencies due to the effects of mass loading and viscous damping. Many efforts have moved away from the conventional Rayleigh mode to other configurations such as STW (surface transverse wave) or Love wave resonators, in which the acoustic energy is guided in a surface film. Others have compared the sensitivity of Rayleigh and Love sensors for varying film parameters in gas sensing experiments [9]. Their results indicated that Rayleigh sensors are suitable for thicker and softer coatings whereas the transverse wave sensors are appropriate for thinner more rigid films (e.g. vacuum deposited Parylene C). In our work, we tested devices fabricated on several lithium niobate substrates: Y-Z (Y rotated Z propagating), 128° Y-X, and 64° Y-X. The latter rotated cut produces surface-skimming bulk waves with in-plane shear polarization. In this way we also tested surface transverse modes. These modes also afford the highest operating frequency for a given wavelength.

Our fabrication procedure is nearly identical to a previous report [10]. In this recent design, our revisions were primarily intended to decrease required antenna size and increase measurement sensitivity. Others have shown the relations for sensitivity in terms of time delay, phase, etc. [11]. The key relationship is given in equation 1. It is apparent that the sensitivity of the total delay (τ) to a perturbing quantity (X) is proportional to the nominal delay (τ_0; equation 2). The abbreviation "XCD" represents the "coefficient of delay" for a quantity X. At a given operating frequency, sensitivity ($\mathrm{S_X}$) to X is therefore increased by subjecting the wave to a particular perturbation for a greater period of time.

$$\tau(\mathrm{X}) = \tau_0(1 + \mathrm{XCD} \cdot \mathrm{X}) \tag{1}$$

$$\mathrm{S_X} = \frac{\partial \tau}{\partial \mathrm{X}} = \tau_0 \cdot \mathrm{XCD} \tag{2}$$

Our three primary design criteria were: (1) to increase the frequency, (2) to increase the transducer bandwidth, and (3) to increase the delays. To do this we have more than doubled the operating center frequency and transducer bandwidth, and we increased the separation distances between transducer and reflectors. The result is shown in figure 2.

The above SAW RFID device produced the pulse response shown in figure 3. The multiple echoes are clearly discerned as variations of the reflection as measured by a vector network analyzer (VNA). The effect of a surface coating is also shown. In a subsequent section we examine such responses for functionalized sensor devices.

III. Methods

A. Chemisensitive Surface Coating

Researchers have already demonstrated polybutadiene (PB) as selective for ozone [12], [5]. One study indicated less than

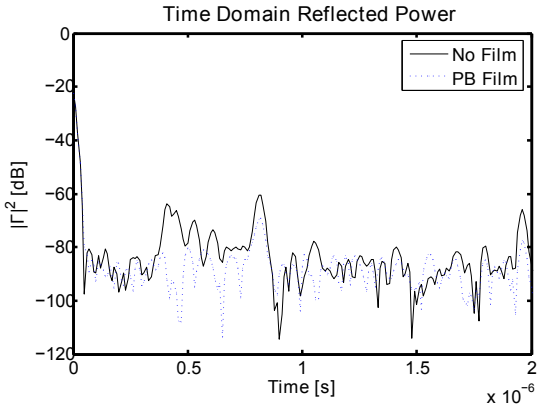

Fig. 3. Temporal reflection magnitude of the 64° Y-X $LiNbO_3$ RFID device of figure 2 at room temperature. The center frequency for this structure is approximaterly 580 MHz.

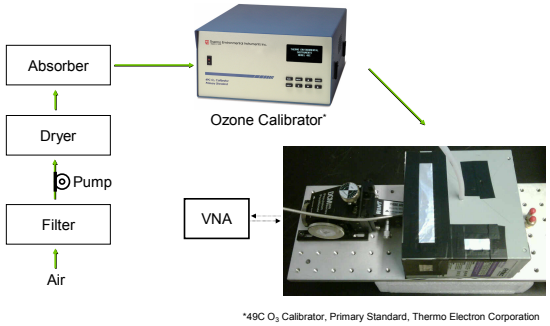

Fig. 4. Schematic of experimental setup. Solid arrows denote sample flow, and dotted arrows indicate electrical interconnect.

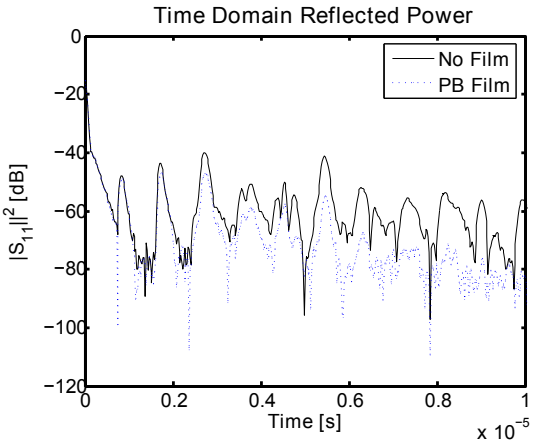

Fig. 5. Time domain responses of a Y-Z $LiNbO_3$SAW RFID device both before and after coating. This substrate demonstrated the strongest acoustic reflections.

6% interference across many other salient gas constituents including: toluene, nitric oxide, and relative humidity. Water vapor and solvent absorption are important factors affecting acoustic properties of polymer films, so the relatively low interference makes this PB film a good choice.

In a prior study, we verified the mass increase in the coating after ozone exposure [6]. In that study, we applied two techniques. The first was x-ray photoelectron spectroscopy (XPS), which indicated a decrease in carbon double bonds and an increase in carbonyl groups, i.e. carbon bonded to oxygen. Our second measurement employed acoustic gravimetric detection of ozone using 10 MHz quartz crystal microbalance (QCM) devices. We reported 2.3 Hz min^{-1} at 100 ppb ozone, and others before us have demonstrated similar results [12].

In the present study, we coated our SAW devices with a similar solution of 5000 molecular weight polybutadiene obtained from Scientific Polymer Products, Inc. The PB was dissolved in toluene to 5% weight and filtered through 0.2 μm syringe filters. Finally, the solution was deposited directly onto devices and spun at approximately 5600 RPM for 60 seconds. We obtained film thickness less than 300 nm using this method.

In undiluted form the polybutadiene was a viscous liquid at room temperature and pressure. Even after solvent evaporation, we expect the film still exhibits a high viscosity. Acoustic measurements on Rayleigh mode resonators confirmed this; the responses were squelched. Even the STW RFID devices did not work with that coating. To solidify the thin films, we bake them between 30 minutes and 2 hours at 110 °C. Thicker films require longer bake times. The baking step accomplishes two primary objectives: (1) to decrease the viscosity of the film (and accompanying acoustic losses) by solvent bake-out, and (2) to stiffen the film by cross-linking. We demonstrate the success of this approach in a subsequent section.

B. Ozone Challenge

The test air stream was conditioned as shown in Figure 4. Ambient room air was drawn through a filter into a pump and delivered to the Thermo Electron Inc. ozone calibrator unit (Primary Standard) after passing through a DrieRite desiccant dryer and an activated carbon filter. The calibrator's outlet was connected by 1/4 inch polyethylene tubing to the aluminum and steel box which housed the sensor(s). The gas flow rate was 3.70 SLPM, as measured with a DryCal DC-2 flow calibrator (BIOS International).

C. RF Measurement

For the initial measurements, we used a Cascade Microtech probe station and an HP8753C network analyzer to electrically characterize the RFID SAW devices. For temperature measurements we used a Temptronic temperature controller connected to the probe station vacuum chuck. The specific RF measurement we use is the frequency-dependent 1-port scattering parameter, $S_{11}(\omega)$. A typical device response is shown later in Figure 8. Though reflections are manifest as ripples in the response passband, time-domain conversion (inverse Fourier transform of $S_{11}(\omega)$) reveals the multiple-echo RFID response one expects (refer to Figure 5).

For ozone measurements, we designed a LABVIEW (National Instruments) program to record $S_{11}(\omega)$ responses to file

every 10 seconds. For device and coating characterization, this arrangement allows observation of the full response (both magnitude and phase versus frequency) over the course of each ozone exposure trial. Subsequent processing in MATLAB (Mathworks) produced the temporal pulse response.

IV. Results & Discussion

A. Film Uniformity

A non-uniform film scatters the surface acoustic wave. This was evident in other work on the functionalization of SAW sensors [13]. The surface preparation must be uniform to within a fraction of one wavelength, and so this challenge becomes more difficult at higher frequencies.

For deposition of extremely thin polymer films, plasma cleaning and conformal silica coating have been used to improve homogeneity of sensing films since at least 1995 [14]. We adopted this technique but found it unnecessary for coating lithium niobate devices with polybutadiene. Cleaning and dehydration of the wafer surface were sufficient. On quartz substrates we did observe "dewetting" of the nonpolar films as the solvent evaporated and the film contracted anisotropically along the surface electrodes and reflectors.

The "dewetting" behavior occurred to some extent on most substrates with polar surfaces. This was especially troublesome on quartz or silica-coated lithium niobate. Our primary solution to this problem was to bake (and thereby dehydrate) the devices prior to coating. Application of a nonpolar surface coating (e.g. HMDS) also reduced the phenomenon but this added a processing step which we found can be avoided for lithium niobate devices by simply baking prior to coating.

B. Film Chemistry

The film mass is increased by irreversible attack of available alkene bonds, and deposited mass (oxygen) corresponds to useful life. Even after baking the films for two hours, our previous QCM trials demonstrated ozone detection both above and below the regulatory ranges. Further demonstration of the film's tolerance to baking is evident by more recent trials in which we baked the films overnight at approximately 200 °C. While the ozone sensitivity was not significantly reduced, the sensor lifetime decreased. This indicates a decrease in double bonds available for reaction. Literature indicates the alkene (π) bond is relatively stable below 300 °C [15]. Even at lower temperatures the alkene bonds of the PB film may very slowly become saturated, making a more rigid film. This saturation process reduces the film's reactive capacity and we suggest it happens, albeit slowly, at lower temperatures. We have not, however, observed consequences of this effect experimentally, including tests run more than 48 hours at room temperature (20 ± 2 °C). In open-air shelf life tests, we found only slight reduction in sensitivity and useful life after two weeks of storage in ambient air at room temperature. For best results, we suggest baking and storing the coated devices in an inert atmosphere and at moderate temperature.

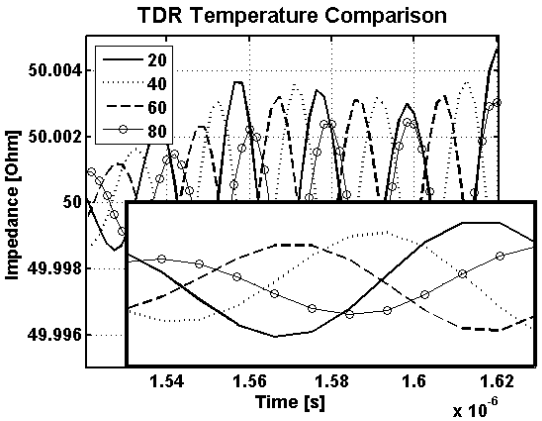

Fig. 6. Phase response of RFID sensor versus time for several temperatures. The center frequency for these devices was approximately 490 MHz. The inset shows the clear separation of phases, while the main frame shows the magnitude varies significantly according to the envelope.

C. Temperature Response

Lithium niobate substrates have temperature coefficients of delay (TCD) of approximately -50 to -80 ppm/°C, as we and others have reported [10]. We compared the phases of echoes returned from the SAW RFID devices and quantified phase shift sensitivity of about 5° per degree Celsius.

The responses shown in Figure 6 are not averages but agree well with several measurements taken at each temperature over the course of several temperature cycles. The phases of all measurements at each temperature were sufficiently identical to eliminate concern of hysteresis or other potential ambiguities. The inset shows more clearly the clear separation of phases over a 60 degree span. The impedance plot reveals the phase whereas the logarithmic magnitude plot does not. We calculate the impedance using the standard equation (3) for normalized S-parameters, with $\mathrm{Z}_0 = 50\ \Omega$. The impedance deviates very little from 50 Ω due to the small perturbation presented by each surface electrode.

$$\mathrm{Z}(t) = \mathrm{Z}_0 \frac{1 + S_{11}(t)}{1 - S_{11}(t)} \tag{3}$$

D. Ozone Response

1) SAW Resonator Confirmation: Following our previous study, we tested 250 MHz STW *resonators* fabricated in our lab at Georgia Tech. The devices employed "ST" cut quartz (having near zero temperature coefficient), and the propagation direction was rotated 90 degrees about the surface normal to achieve SSBW/STW polarization [16]. This configuration is known to reduce damping effects due to liquid or polymer coatings because the acoustic wave has shear polarization in the plane of the sensor surface.

A SAW PRO-250 oscillator unit allowed measurement of the resonant frequency at one second intervals. This was beneficial for validation of the film preparation for use at high frequencies. The experiment also enabled assessment of the

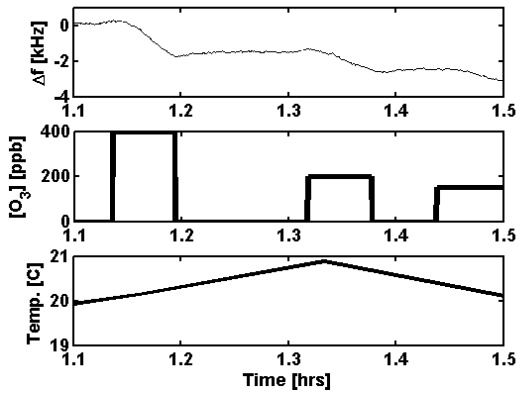

Fig. 7. Response of a 250 MHz SAW resonator to ozone challenges.

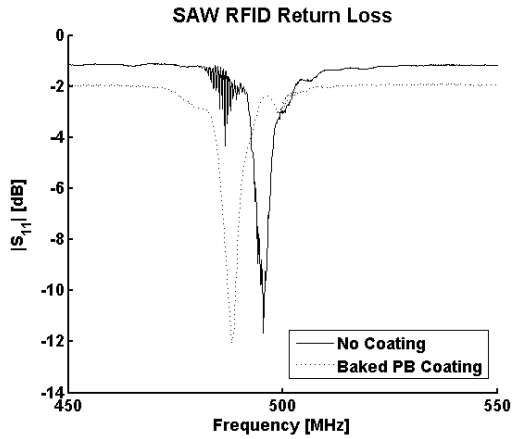

Fig. 8. Comparison of frequency domain return loss for a Rayleigh mode device before and after coated with polybutadiene.

response time to the ozone challenges, as outlined in Figure 7. The sensor responded almost immediately on the time scale of minutes, and the sensitivity averaged -1.70 Hz min^{-1} ppb^{-1}, with a standard deviation of 0.076 Hz min^{-1} ppb^{-1} over 4 trials at different concentrations.

Our success with the SAW resonators implies the functionalization protocol is successful for high frequency SAW devices when the loss is acceptably low. The resonators were operated in an oscillator loop, and the devices exhibited a high quality factor, Q, of several thousand. Whereas many cite the Q of *resonator* sensors, this measure is not often applied to SAW RFID sensors which are typically *broadband* devices. Rather, an equivalent definition of Q can be achieved using a formula given by equation 4 [17].

$$\mathrm{Q} = 2\pi \mathrm{f}_0 \frac{\tau}{2} = \pi \mathrm{f}_0 \tau \tag{4}$$

Letting f_0 be the device center frequency (550 MHz, determined from $\mathrm{S}_{11}(\omega)$) and τ (470 nanoseconds, determined from figure 9) we estimated the equivalent Q for our STW device is approximately 840. We define τ as the length of time, such as the traditional group delay or ringing time, for which the acoustic waves are useful within the structure.

2) SAW RFID Measurements: The SAW RFID sensors were characterized both before and after the PB coating procedure. We measured the return loss and compared the responses, e.g. figure 8. The figure demonstrates absolute reduction in energy transfer (more return loss), and the passband ripples are notably absent (at the lower frequency "shoulder") implying the reflections are greatly damped. In the temporal plots (e.g. figure 5), one can see the individual reflections are damped by about 10 dB.

A SAW RFID ozone trial was performed using the 580 MHz STW substrate. The device was a simple reflective delay line structure without multiple ID encoding reflections. We recorded full one-port scattering parameters every 10 seconds using the software automation described prior. The sampling rate was regular, allowing us to see the response $\Re(S_{11}(t))$ advanced more rapidly during ozone exposure. Figure 9 clearly shows this effect. The contour lines representing regular acquisition intervals are farthest apart in the middle experiment times, i.e. during exposure to ozone at 180 ppb. We calculated the response to be -7.6 ps min^{-1} ppb^{-1}. In fact, unlike any of the other devices tested, the shear horizontal (STW) device actually demonstrates an increase in acoustic phase velocity due to the reaction in the film.

Though the sensitivity to ozone was quite low by comparison to temperature measurements, we can attribute this to at least two things. First, the delay was not made as large as that used in the temperature experiments. Thus, as given in equation 2, the delay sensitivity was necessarily lower because the nominal delay, τ_0, was about ten times less (600 μm versus 6000 μm). Second, the STW mode was employed, and its character is known to be highly dependent upon the thickness.

V. Conclusion

We have prepared submicron polybutadiene coatings and demonstrated their sensitivity to ozone of varying concentration using quartz crystal microbalances at 10 MHz and SAW resonators at 250 MHz. We subsequently coated both SAW resonators and SAW RFID devices, showing that lithium niobate is not only advantageous for its high piezoelectric coupling, but also for its surface compatibility with polybutadiene coatings.

Because the sensitivity of delay-based SAW RFID temperature and ozone measurements is proportional to the echo delay, we have explored the reduction of propagation loss for coated devices. After comparison of loading characteristics for different film preparations and crystal cuts, we determined Y-Z $LiNbO_3$ gave best results, allowing echo delays greater than 5 microseconds for surface functionalized devices.

Temperature measurements revealed the necessity of phase information for discerning ppm changes in SAW velocity due to temperature. Finally, we quantified ozone sensitivity for STW SAW devices on 64° Y-rotated X-propagating lithium niobate. We compared the phases of one-port scattering parameter measurements through the course of ozone exposure.

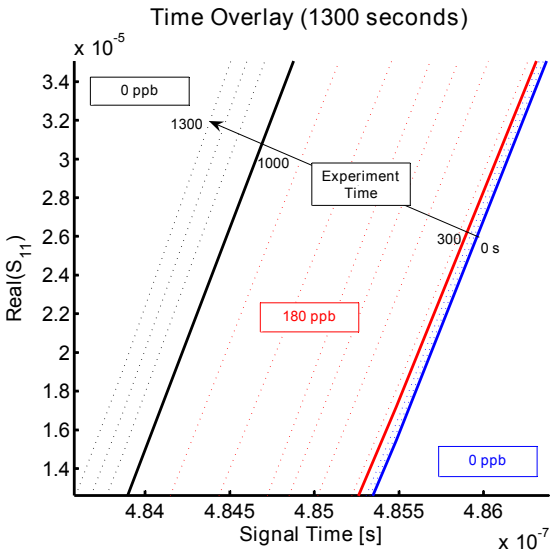

Fig. 9. Solid lines denote the start of each phase of the experiment. The signal time was produced from the frequency-dependent one-port scattering parameter. The experiment phases prior to (right) and after ozone exposure (left) were approximately five minutes' duration.

We then determined the sensitivity could be improved by increasing the distance between transducer and reflector and by decreasing the loss in the film itself.

ACKNOWLEDGMENT

The authors would like to thank John Kangchun Perng for performing the mask layout.

This work was supported by the National Science Foundation under contract no. ECS-0524255 (L. Lunardi) and the Office of Naval Research under contract no. 21066WK (M. Specter).

REFERENCES

[1] K. Lee, W. Wang, T. Kim, and S. Yang, "A novel 440 mhz wireless saw microsensor integrated with pressure-temperature sensors and id tag," *Journal of Micromechanics and Microengineering*, vol. 17, no. 3, pp. 515–523, 2007. [Online]. Available: http://stacks.iop.org/0960-1317/17/515

[2] W. Kohmyr, R. Grass, and R. Leonard, "Dobson Spectrophotometer-83 - a standard for total ozone measurements, 1962-1987," *JOURNAL OF GEOPHYSICAL RESEARCH-ATMOSPHERES*, vol. 94, no. D7, pp. 9847–9861, JUL 20 1989.

[3] J. Kerr, "Understanding the factors that affect surface ultraviolet radiation," *OPTICAL ENGINEERING*, vol. 44, no. 4, APR 2005.

[4] S. Winiecki and J. Frederick, "Ultraviolet radiation and clouds: Couplings to tropospheric air quality," *JOURNAL OF GEOPHYSICAL RESEARCH-ATMOSPHERES*, vol. 110, no. D22, NOV 16 2005.

[5] H. FOG and B. RIETZ, "PIEZOELECTRIC CRYSTAL DETECTOR FOR THE MONITORING OF OZONE IN WORKING ENVIRONMENTS," *ANALYTICAL CHEMISTRY*, vol. 57, no. 13, pp. 2634–2638, 1985.

[6] R. S. Westafer, G. Levitin, D. W. Hess, M. H. Bergin, P. J. Edmonson, and W. D. Hunt, "Ozone sensors for real-time passive wireless application," in *EPA International Environmental Nanotechnology Conference*, Oct. 2008.

[7] C. Hartmann, "A global saw id tag with large data capacity," in *Ultrasonics Symposium, 2002. Proceedings. 2002 IEEE*, vol. 1, Oct. 2002, pp. 65–69 vol.1.

[8] A. Polh, "A review of wireless saw sensors," *Ultrasonics, Ferroelectrics and Frequency Control, IEEE Transactions on*, vol. 47, no. 2, pp. 317–332, Mar 2000.

[9] I. Avramov, M. Rapp, S. Kurosawa, P. Krawczak, and E. Radeva, "Gas sensitivity comparison of polymer coated saw and stw resonators operating at the same acoustic wave length," *Sensors Journal, IEEE*, vol. 2, no. 3, pp. 150–159, Jun 2002.

[10] J. Perng, W. Hunt, and P. Edmonson, "Development of a shear horizontal saw rfid biosensor," in *Sensors, 2007 IEEE*, Oct. 2007, pp. 691–694.

[11] J. Kuypers, L. Reindl, S. Tanaka, and M. Esashi, "Maximum accuracy evaluation scheme for wireless saw delay-line sensors," *Ultrasonics, Ferroelectrics and Frequency Control, IEEE Transactions on*, vol. 55, no. 7, pp. 1640–1652, July 2008.

[12] D. Black, R. Harley, S. Hering, and M. Stolzenburg, "A new, portable, real-time ozone monitor," *ENVIRONMENTAL SCIENCE & TECHNOLOGY*, vol. 34, no. 14, pp. 3031–3040, JUL 15 2000.

[13] S. H. Lee, E. Massey, R. Westafer, and W. Hunt, "A novel method to investigate dependence of saw resonator sensor signatures on localized surface perturbations," in *Sensors, 2006. 5th IEEE Conference on*, Oct. 2006, pp. 1203–1206.

[14] J. W. Grate and R. A. McGill, "Dewetting effects on polymer-coated surface acoustic wave vapor sensors," *Analytical Chemistry*, vol. 67, no. 21, pp. 4015–4019, 11 1995. [Online]. Available: http://dx.doi.org/10.1021/ac00117a031

[15] Vollhardt and Shore, *Organic Chemistry*, 4th ed. W. H. Freeman, 2002, pp. 436–438.

[16] D. Thompson and B. Auld, "Surface transverse wave propagation under metal strip gratings," in *IEEE 1986 Ultrasonics Symposium*, 1986, pp. 261–266.

[17] C. Campbell, *Surface Acoustic Wave Devices for Mobile and Wireless Communications*. Academic Press, 1998, p. 601.